Advances in reflection grating technology for Constellation-X

Ralf K. Heilmann, Mireille Akilian, Chih-Hao Chang, Carl G. Chen, Craig R. Forest, Chulmin Joo, Paul T. Konkola, Juan C. Montoya, Yanxia Sun, Jenny You, and Mark L. Schattenburg

Space Nanotechnology Laboratory, Center for Space Research,
Massachusetts Institute of Technology,
77 Massachusetts Avenue, Cambridge, Massachusetts 02139, USA

ABSTRACT

The Reflection Grating Spectrometer (RGS) on Constellation-X will require thousands of large gratings with very exacting tolerances. Two types of grating geometries have been proposed. In-plane gratings have low ruling densities ($\sim$ 500 l/mm) and very tight flatness and assembly tolerances. Off-plane gratings require much higher ruling densities ($\sim$ 5000 l/mm), but have somewhat relaxed flatness and assembly tolerances and offer the potential of higher resolution and efficiency. The trade-offs between these designs are complex and are currently being studied. To help address critical issues of manufacturability we are developing a number of novel technologies for shaping, assembling, and patterning large-area reflection gratings that are amenable to low-cost manufacturing. In particular, we report results of improved methods for patterning the sawtooth grating lines that are required for efficient blazing, including the use of anisotropic etching of specially-cut silicon wafers to pattern atomically smooth grating facets. We also report on the results of using nanoimprint lithography as a potential means for replicating sawtooth grating masters. Our Nanoruler scanning beam interference lithography tool allows us to pattern large area gratings up to 300 mm in diameter. We also report on developments in grating assembly technology utilizing lithographically patterned and micromachined silicon metrology structures ("microcombs") that have achieved submicron assembly repeatability.

Keywords: x-ray optics, Constellation-X, in-plane gratings, off-plane gratings, reflection gratings, blaze, sawtooth, replication, nanoimprint lithography, microcomb

1. INTRODUCTION

Constellation-X is the next major x-ray telescope planned by NASA. Complementing Chandra's exquisite spatial resolution,[1] it is designed with a much higher effective collecting area of at least 700 to 2,500 cm^2 and a spectral resolving power of at least 300 over the soft x-ray bandpass (0.25 to 2 keV).[2] This energy range is primarily covered by the Reflection Grating Spectrometer (RGS), an array of reflection gratings placed at grazing incidence into the converging beam downstream of the imaging mirror assembly, the Spectroscopy X-ray Telescope (SXT).

To achieve the required collecting area the gratings will cover 57% of the area intercepted by the SXT. Due to the small grazing angle of incidence onto the gratings this results in a grating area of roughly 100 m^2, about the size of one side of a volleyball court. Assuming a grating size of 100×140 mm^2 per individual grating, at least 7000 gratings have to be manufactured. At the same time the mass of the RGS should be on the order of 50 kg. This large area-to-mass ratio requires the grating substrates to assume a thin foil-like shape with a foil thickness around 500 microns.

In order to meet resolution goals these foils have to be flat to better than 2 arcsec (or $\sim$ 0.5 micron for low spatial frequency figure errors), and aligned with respect to each other with the same precision. To avoid having to mount and align thousands of gratings individually we follow a modular approach, where tens of gratings each are assembled and aligned together in identical flight modules, and the modules are subsequently mounted and aligned to a common support structure.

In the following sections we review recent progress in our laboratory in several areas instrumental to the RGS technology development. We first present the results of accuracy tests on our foil optic assembly truss.

Further author information: Send correspondence to R.K.H. E-mail: ralf@space.mit.edu, URL: http://snl.mit.edu/

Optics for EUV, X-Ray, and Gamma-Ray Astronomy, edited by Oberto Citterio, Stephen L. O'Dell, Proceedings of SPIE Vol. 5168 (SPIE, Bellingham, WA 2004)
0277-786X/04/$15 · doi: 10.1117/12.510258

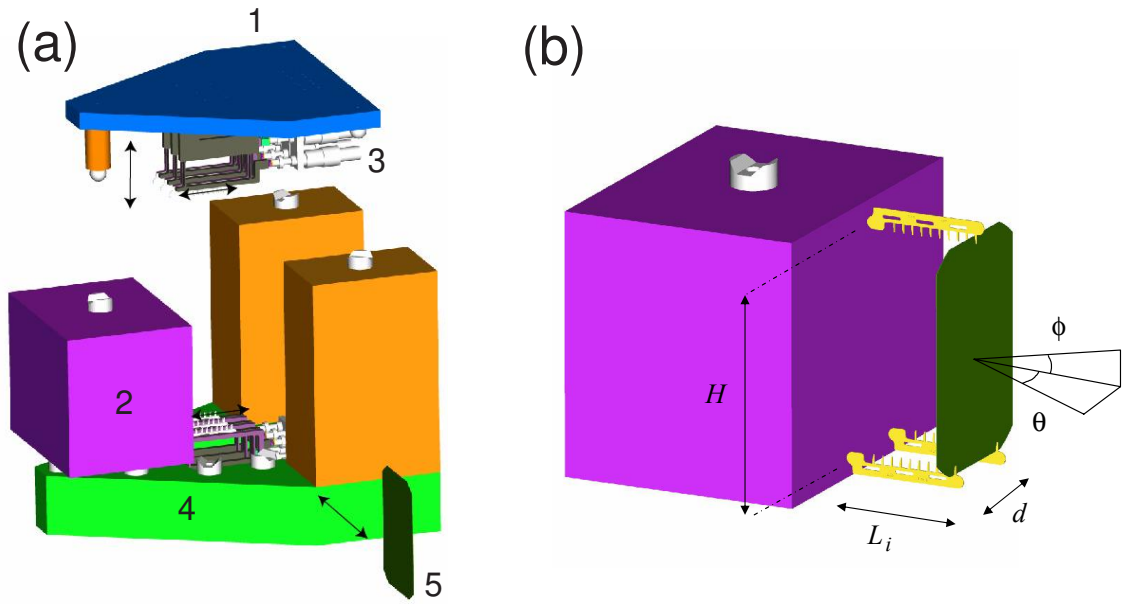

Figure 1. Assembly truss schematic. (a) Exploded view, showing disassembly during dynamic repeatability tests. The labeled parts are lid (1), reference block (2), top flexure bearing assembly (3), base (4), and a foil optic (5). (b) Accuracy testing schematic, showing a foil positioned by three microcombs and its yaw (Θ)and pitch (Φ) angles relative to the reference surface. $H = 140$ mm and $d = 55$ mm.

The assembly truss together with micromachined silicon alignment bars - the so-called microcombs - form the metrology frame necessary for alignment and assembly of foils into modules. The process to fabricate the microcombs has undergone a number of improvements and is described next. Previously we had manufactured high efficiency reflection gratings for the in-plane geometry. Below we present our latest results in patterning efficient blazed gratings for the off-plane mount. We then report results on using nanoimprint lithography to fabricate replicas from these gratings. Finally we acquaint the reader with our Nanoruler tool that enables us to cover substrates of up to 300 mm diameter with a sub-micron period, nanometer phase-coherent grating in under one hour.

2. ASSEMBLY TRUSS ACCURACY TESTS

We have designed and built a second generation assembly truss to perform and study the alignment of foil optics parallel to each other within a module to tolerances compatible with the 2 arcsec resolution goal.[3,4] This corresponds to repeatably and accurately placing the front faces of the foils to within 1 μm of their ideal positions. The assembly truss features a reference flat (1 μm flatness peak-to-valley), kinematic couplings between base, lid, reference flat, and flight module, and a force-sensor-equipped flexure bearing assembly that supports actuation of the microcombs against the reference flat (see Fig. 1(a)). The design effectively separates metrology frame, assembly tool mechanical structure, and flight module, which limits the most stringent requirements to the reusable components of the metrology frame and relaxes manufacturing tolerances for the many flight modules. The microcombs come in two varieties. Reference combs establish the distance between foil optic front surfaces and the reference surface, while spring combs hold the foils against the teeth of the reference combs.

Briefly, the envisioned assembly procedure proceeds as follows: First the slightly oversized slots of an empty flight module are populated with foil optics. Assembly truss and microcombs are then assembled with the flight module placed inside the assembly truss. Next the reference combs are actuated against the reference flat with a calibrated force, and then the spring combs are used to push the foils into contact with the reference combs' teeth. With the foils now accurately held in their desired positions they are glued to the flight module. Once the glue is cured the microcombs are retracted, the lid is taken off, and the populated flight module is removed.

Table 1. Assembly truss slot accuracy results. *Displacement error* is the relative displacement of the foil edge from an ideal position, deduced from the foil's dimensions and systematic angular errors in pitch (Φ_s) and yaw (Θ_s). Errors for three successive slots are shown together with average systematic errors. See also Fig. 1.

Displacement error [μm]	Yaw (Θ_s)	Pitch (Φ_s)
Slot 1	0.56	-1.84
Slot 2	0.25	-1.84
Slot 3	0.21	-2.34
Avg.	0.34	-2.01

A number of tests of the assembly truss have been described previously.[3, 4] Dynamic tests that involve complete dis- and reassembly of the assembly truss to mimic the above assembly procedure have been performed. The angle of a single optic with respect to the reference flat was measured with an autocollimator, from which relative displacements of the foil edges were deduced. We found the placement of the optic to be repeatable to 1/3 of a micron (one sigma), which already meets our goals. We suspect that some fraction of this small repeatability error is due to imperfections in our metrology (manual autocollimator readout) and lack of temperature control ($\Delta T \simeq 7^o$ C over one day) and are currently investigating these issues.

Testing of the foil placement accuracy was complicated by temporary microcomb fabrication problems, leading to inaccurate microcomb dimensions. We believe that we have solved these problems with the process improvements described in Section 3. In our accuracy tests we measure pitch and yaw of the foil optic relative to the reference flat (see Fig. 1(b)) with an autocollimator. In order to subtract out possible errors due to the microcombs we performed measurements with six possible permutations of the flexure bearing assemblies (with the microcombs attached to them). At each permutation the foil optic was placed into three different slots on the microcombs. The accuracy results from these measurements are listed in Table 1.[3] The error budget predicts assembly accuracy of 0.5 μm in pitch and yaw, assuming that systematic errors can be measured and compensated for. The observed error in yaw is smaller than predicted (0.34 μm or 1.13 arcsec), while we find a systematic linear error of about 2 μm (2.95 arcsec systematic angular error) in pitch. Possible contributions to that error are due to the 1 μm (P-V) flatness of the reference flat and the 2 μm (P-V) flatness of the test optic - a $3 \times 100 \times 140$ mm^3 quartz plate with a reflective coating. With tighter flatness specifications we expect the pitch error to become as small as the observed error in yaw.

3. MICROCOMB FABRICATION

Dimensional accuracy is crucial to the alignment of grazing-incidence optics on the scale of current x-ray telescopes. In addition, a large number of optics needs to be aligned, since the required total optics area is about 40 times the desired effective collection area. As outlined above it is desirable to align as many reflection gratings as possible in a single step. Microcombs were designed with sub-micron dimensional accuracy and "gang-alignment" of foil optics in mind. Their basic *modus operandi* is schematically shown in Fig. 2.

In order to achieve the best possible dimensional accuracy, microcombs are fabricated using micro-electro-mechanical systems (MEMS) technology.[5] The microcombs' dimensions directly derive from the placement of foil optics in the telescope design. The mechanical design and other properties of the microcombs have been described previously.[5–9]

The microcomb pattern is exposed through a mask onto a resist and silicon dioxide covered silicon wafer. After resist development the wafer is plasma-etched all the way through via deep reactive-ion etching (DRIE). Loss in dimensional accuracy can be due to a low resolution mask making process, errors in pattern transfer from mask to resist, and etch process imperfections. Currently inaccuracies are dominated by the latter source, which is why we focused on process improvements first.[10]

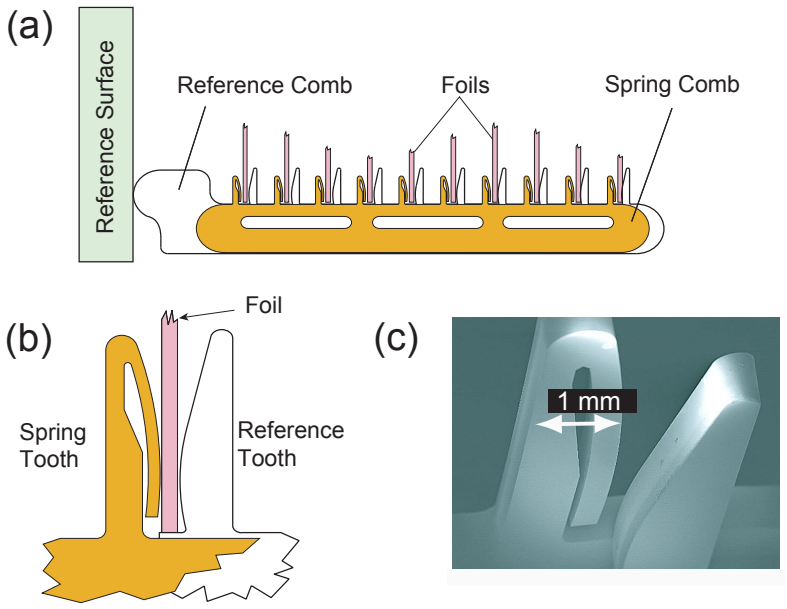

Figure 2. Microcomb schematic. (a) The reference comb is in contact with the reference surface. The spring comb holds foils against reference teeth. (b) Enlarged view of spring and reference tooth pair, holding a foil between them. (c) SEM of an actual spring and reference tooth pair.

Our main interest is in position accuracy, which we define as the relative placement of the tooth-to-foil contact points and their placement with respect to the microcomb-to-reference-flat contact point. We can therefore tolerate loss in dimensional accuracy, as long as it is uniform over the whole wafer.

Position accuracy of better than 1 μm has been demonstrated previously by etching through a double-side polished, 380 μm thick, 100 mm diameter silicon wafer.[5] However, the size of a wafer limits the length of the microcombs. It is therefore desirable to manufacture the combs from larger - and thus generally thicker - wafers. This leads to two problems. First, our current DRIE facility has poor etch rate uniformity over the area of a 150 mm diameter wafer, and second, the larger thickness (500 μm) requires longer etch times, which in turn amplifies etch rate variations, leading to variations in mask erosion and undercutting. Etch rate variations also require overetching in some areas, which can lead to increased sidewall roughness and micrometer scale defects.[10]

In order to mitigate the effects of etch rate variations we developed a double-side etch process, using a silicon-on-insulator (SOI) wafer and two separate masks, schematically shown in Fig. 3. The first mask has wider trenches and is used to etch the wafer from the back all the way to the 2 μm thick buried silicon oxide (BOX) layer, which serves as an etch stop and can withstand 15 minutes of overetch. The back side features are not critical, since they will neither be in contact with the foil optics, nor the reference flat. The front side ("device layer") is patterned with the second mask, which contains the dimensionally accurate features. In our case the device layer is only 100 μm thick. The resulting short etch time efficiently minimizes the detrimental effects of etch rate variations on the front side features. The remaining oxide layer can then be removed with a buffered-oxide etch (BOE).[10] Fig. 4 shows a typical resulting trench etched through the wafer.

This process is robust and expected to increase the microcomb fabrication yield. Its accuracy is primarily determined by the device layer thickness and therefore should be applicable to even thicker wafers.

4. FABRICATION OF BLAZED GRATINGS FOR THE OFF-PLANE GEOMETRY

Blazed gratings diffract very efficiently when the conditions of specular reflection from a facet and the grating equation are fulfilled simultaneously.[11] For a given geometry this allows a certain degree of optimization for diffracting efficiently into a desired diffraction order. For efficient x-ray reflection gratings the grazing angle of

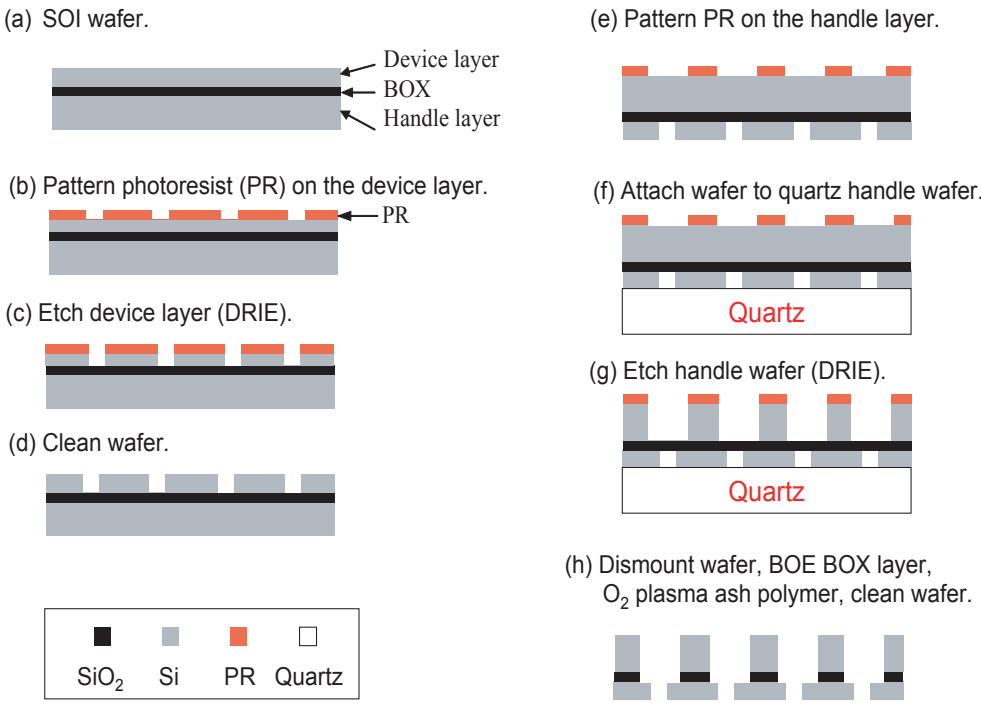

Figure 3. Schematic of the double-side etch microcomb fabrication process on a SOI wafer. In our case the device layer thickness is 100 μm $\pm$1 μm, the BOX layer is 2 μm thick, and the handle layer is 350 μm $\pm$5 μm thick.

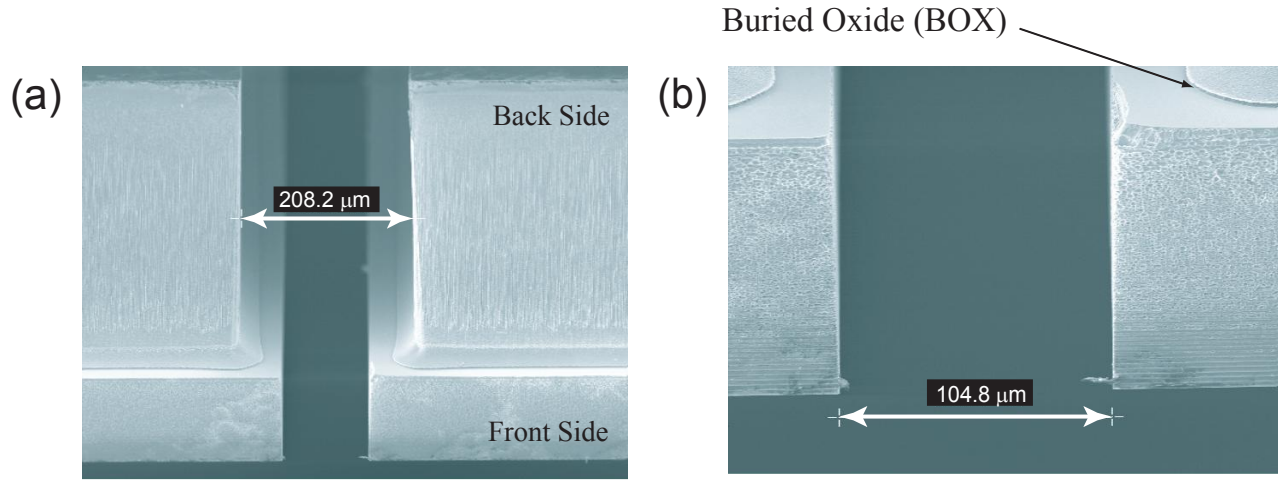

Figure 4. Scanning electron micrographs of a double-side etched trench on a SOI wafer. The masks have trench widths of 100 μm (front side) and 200 μm (back side), respectively. (a) Low magnification. (b) High magnification. The BOX layer is barely visible.

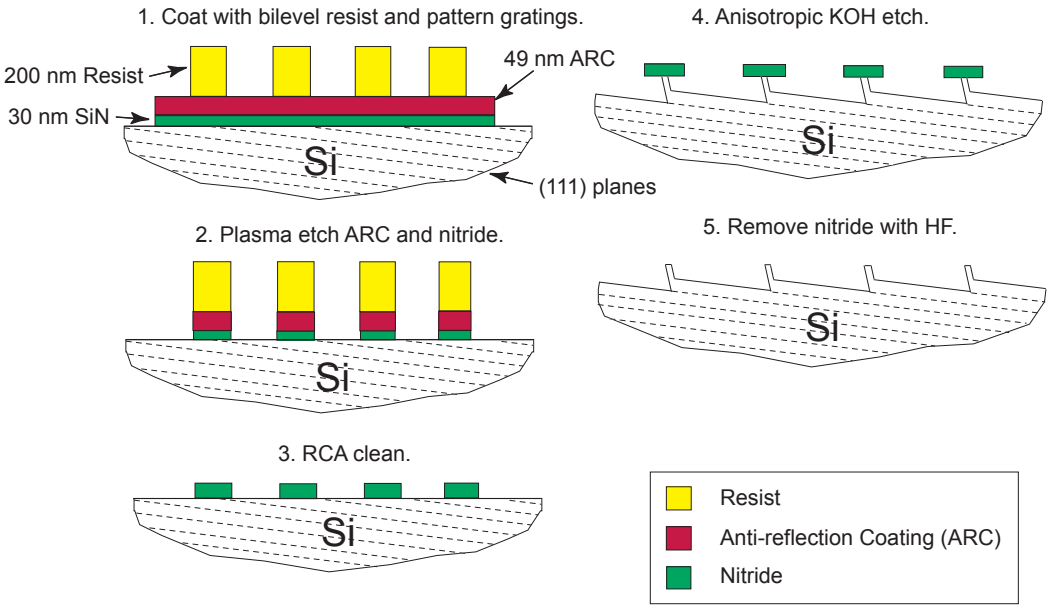

Figure 5. Fabrication process for 200 nm period grating with 7^o blaze angle. The dashed lines in the silicon substrate symbolize the (111) lattice planes.

incidence is limited by the critical angle of total external reflection, which is typically on the order of 2 degrees or less. This leaves grating period, blaze angle, and direction of the grating vector relative to the plane of incidence as the main parameters to vary. The in-plane geometry (classical mount) has the grating vector in the plane of incidence, while in the extreme off-plane or conical geometry[12] or GMS mount[13] the grating vector is almost normal to the plane of incidence. The former case is realized in the RGS of the Newton-XMM x-ray telescope,[14] where the gratings were replicated through a multi-generation replication tree from mechanically ruled masters. The off-plane geometry promises roughly twice the groove efficiency,[12,13,15] but requires much steeper blaze angles and much higher line densities for comparable angular resolution, pushing the limits of manufacturing technology. There also exists the potential to utilize higher diffraction orders to increase resolution at shorter wavelengths since the conical geometry is subject to less vignetting. These and other aspects are discussed in more detail elsewhere.[16,17]

Mechanical ruling is an extremely slow process and it usually creates rough grating profiles with rounded edges, among other problems. In the past we have successfully fabricated high-efficiency reflection gratings from single-crystal silicon substrates that were intentionally miscut from the (111) plane by the desired blaze angle. They were designed for the in-plane geometry with a period of 1.7 μm and a blaze angle of 0.7^o.[18] While the classical mount has a strong pedigree, to date no systematic studies have been performed on real gratings for the off-plane mount in the energy band relevant to the Constellation-X RGS. And even though the process described by Franke *et al.*[18] produced highly efficient in-plane gratings, it is not a given that it will be equally successful in the off-plane case, where the grating profile has much more topography. Higher line density and steeper facets might give rise to more surface defects, edge rounding during coating, and increased scatter.

We therefore set out to fabricate reflection gratings for the off-plane case. We patterned single-crystal silicon wafers miscut by $7^o \pm 0.5^o$ from the (111) plane by interference lithography (wavelength $\lambda = 351.1$ nm) with a 200 nm period grating. Before patterning the wafer is covered with silicon nitride and a bi-level resist layer, consisting of anti-reflection coating (ARC) and photoresist.[19] The grating lines are parallel to the $[1\bar{1}0]$ direction. After transferring the grating pattern into nitride the substrate is etched in KOH, which anisotropically etches in the direction parallel to the (111) planes, potentially resulting in atomically smooth facets at the desired blaze angle. Finally, the nitride mask is removed in HF (see Fig. 5). Our first few gratings produced this way were coated with a reflective Cr/Au layer and showed outstanding diffraction efficiency in independent x-ray tests

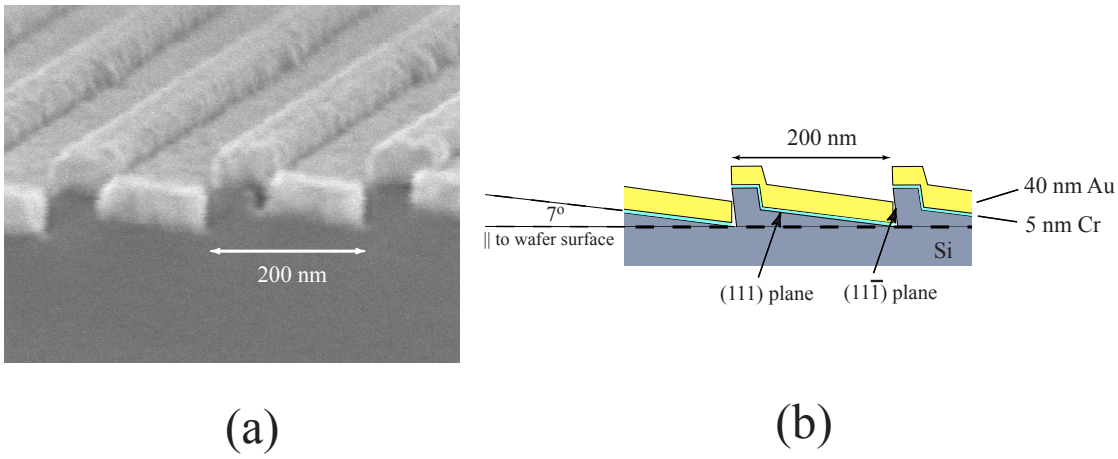

Figure 6. Blazed grating fabricated according to Fig. 5. (a) SEM picture of cleaved grating. (b) Schematic cross section.

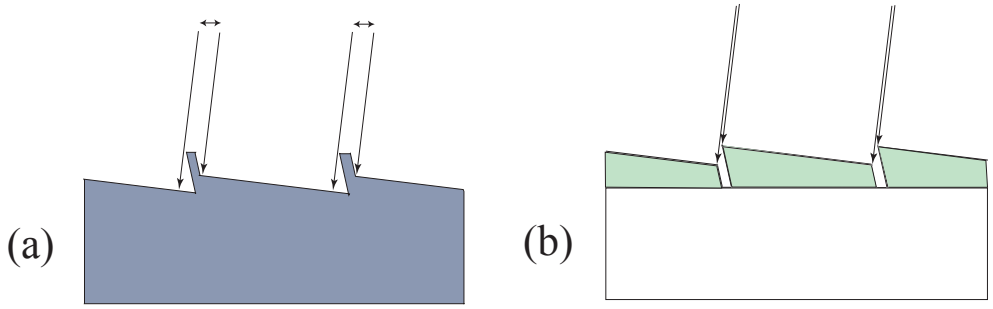

Figure 7. Effect of nubs on blazing efficiency. Long arrows are incident x rays projected onto the plane of the drawing. (a) Nubs on the silicon master are not at the blaze angle, and they partially shadow the blaze facet. The fraction of x rays that hit the nubs do not contribute efficiently to the desired blazing in the diffracted orders. (b) On the replica the nubs turn into troughs. Practically all x rays are incident on the blaze facet.

performed at a gratings test facility at the University of Colorado[20] (see Table 2) and at the Advanced Light Source at Lawrence Berkeley National Laboratory.[21]

As can be seen in Figures 5 and 6 this process leaves silicon nubs protruding between facets. Even though they are less of a problem than in the classical mount, these nubs will reduce the blazing effect and lead to undesired shadowing. The nubs can be minimized through careful linewidth control in the patterning step and controlled KOH etching, or they can be removed completely with additional processing steps.[18]

Facing the task of having to produce thousands of gratings, some method of replicating many gratings from a small number of masters could reduce the patterning and processing effort significantly. One obvious advantage of replication would be that the nubs from the silicon masters "disappear" in the replica, as illustrated in Fig. 7.

Grating replication traditionally involves application of tens-of-microns-thick layers of epoxy to a blank. On large blanks the epoxy thickness can vary by microns, directly affecting the figure. On thin blanks, such as the thin foil optics discussed here, film stress and epoxy shrinkage can lead to shape deformations. Together with potential outgassing problems it is therefore desirable to keep any applied layer as thin as possible.

Nanoimprint lithography (NIL)[23] is a promising technique for the replication of patterns on the nanometer scale. We implemented a novel variation of the so-called step-and-flash imprint lithography (SFIL).[24] We press a silicon grating of area 40×40 mm^2, fabricated as described above, into a low-viscosity UV-curable liquid on a UV transparent substrate (fused silica wafer), using vacuum suction. After curing the liquid via UV exposure

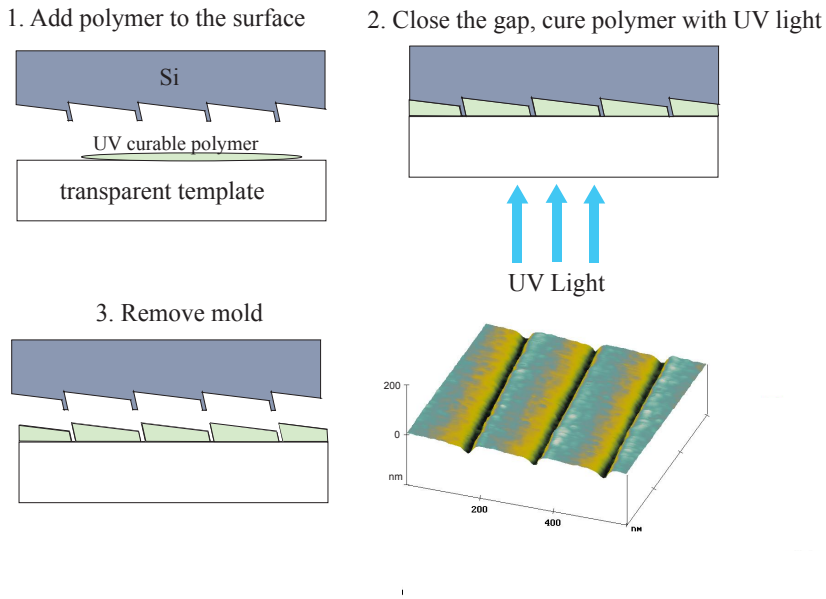

Figure 8. Fabrication of 200 nm period sawtooth replica via SFIL with a transparent substrate. The bottom right shows an AFM image from a replica after coating with 5 nm Cr and 40 nm Au.

Table 2. Preliminary results from recent x-ray diffraction efficiency measurements on Cr/Au coated gratings similar to the one shown in Fig. 6. Measurements were performed following the same procedures as those outlined in Ref. 22. No noticeable scatter was observed even at the highest x-ray energies. $^{(a)}$Range is due to a range of incidence angles.

X-ray energy [keV]	Absolute efficiency: strongest diffracted order	Absolute efficiency: sum diffracted orders	Absolute efficiency: sum (incl. 0 order)
0.277 (C-K)	0.347	0.491	0.561
0.525 (O-K)	0.368	0.574	0.674
0.93 (Cu-L)	0.18-0.21$^{(a)}$	0.29-0.37$^{(a)}$	0.24-0.44$^{(a)}$
1.25 (Mg-K)	0.09-0.31$^{(a)}$	$> 0.24^{(a)}$	0.27-0.53$^{(a)}$

through the substrate, the silicon master and the replica are separated (see Fig. 8). We observe very good feature preservation in the replica with SEM and AFM and no obvious release damage.[19] Recent x-ray diffraction efficiency measurements on our first replicas (coated with Cr/Au) gave very promising results.[21] Some of the questions that need to be answered in the future are how well the features in the master are being replicated, how many good replicas can be made from a single master, and what kind of in- and out-of-plane distortions appear and can be tolerated when replicating larger area gratings. While commercial NIL tools are available for substrate diameters up to 200 mm, we are not aware of any systematic studies of replication induced distortions on these length scales. We are in the process of designing studies to address these issues in collaboration with a number of NIL companies.

5. PATTERNING OF LARGE-AREA GRATINGS WITH THE NANORULER

The 200 nm period gratings described above are patterned with an in-house interference lithography setup that interferes two spherical waves over an area of only $\sim$ 10 cm^2. Interference of spherical waves also leads to undesired hyperbolic deviations from a straight grating pattern.[25] Generating grating patterns of the size

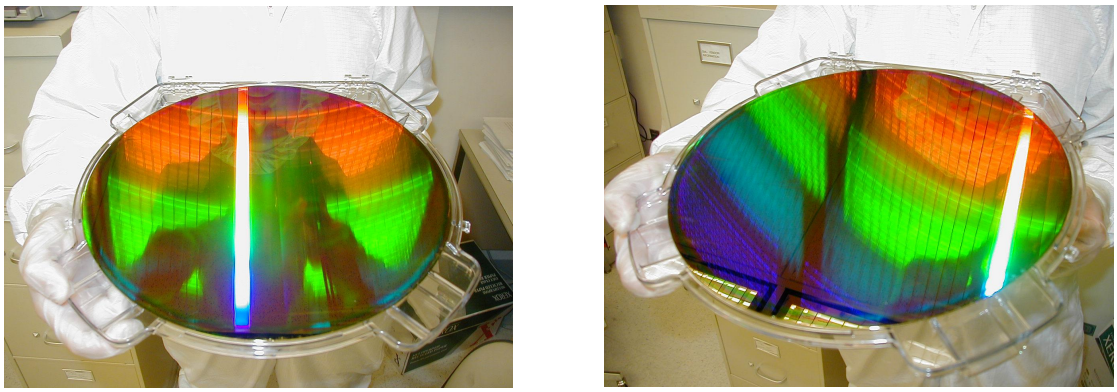

Figure 9. Grating written with the Nanoruler onto a 300 mm diameter silicon wafer. The grating period is 400 nm. (a) The bright stripe down the middle of the wafer is the back diffracted camera flash. Also visible is the back diffracted image of the photographer, and the reflection of the person holding the wafer. The grating lines run left to right. (b) Same as (a), but from a different angle.

required for the Constellation-X RGS with long- and short-range phase distortions of only a small fraction of the grating period is not a trivial task.

Over the last few years we have designed and built a large-area grating patterning tool, called the Nanoruler, based on the technique of scanning-beam interference lithography (SBIL). In SBIL a highly linear grating image is formed through interference of two small (1-2 mm or less) diameter coherent laser beams, and a large resist covered substrate, chucked to an interferometer-controlled x-y air bearing stage, is scanned and stepped through the image grating region. Thus the laser beams "rule" thousands of grating lines with each pass. Between passes the substrate has to be stepped over relative to the image grating by an integer multiple of the grating period with a precision better than a small fraction of the period. The period itself must be known and held constant at the ppm level. Subsequent passes must overlap sufficiently to achieve constant exposure dose across the whole wafer.

Stringent environmental control, refractometry corrections, acousto-optic fringe control, active beam steering, image metrology, a beam alignment system, vibration isolation with feed forward, and careful mechanical and optical design lead to fringe placement stability in the resist of 2.1 nm (3σ), even when scanning at 100 mm/s.[26–34] Wafers of 300 mm diameter are routinely patterned with 400 nm period lines in well under one hour (see Fig. 9). With our current laser ($\lambda = 351.1$ nm) the Nanoruler can write periods down to ~ 200 nm. It can not only be used to pattern large area gratings (writing mode), but also to generate phase maps of existing gratings (reading or metrology mode). We demonstrated mapping repeatability of 2.9 nm (3σ) over a 100 mm wafer.[32,34] This capability allows, for example, to write a master grating, replicate it, and generate a phase map of the coated replica. The phase map gives useful information on in-plane distortions relative to the master, while our Shack-Hartmann wavefront sensor[3,4] characterizes out-of-plane distortions.

The RGS is to be placed downstream from the SXT, where the x rays converge towards the focal point. Due to this convergence the grazing angle of incidence on a flat reflection grating is smaller at the upstream end of the grating than at the downstream end. For a strictly linear grating this would lead to aberrations in the diffracted orders. However, this variation of incidence angle as a function of distance from the focus can be compensated for, to a very high degree, by a change in grating period along the optical axis, resulting in a radial grating.[16,35,36] For example, in the case of a $l = 140$ mm long grating with a nominal period $p = 200$ nm placed directly behind a Wolter mirror with focal length $f = 10$ m the period would change from $p = 200$ nm to $\simeq p(1 - l/f) = 0.986p = 197.2$ nm.

We have previously studied the ability to vary the grating period during SBIL.[37,38] Now that the Nanoruler

is operational and its performance characterized, we are working to add variable-period capability (VP-SBIL), which will allow us to pattern radial gratings for the off-plane geometry or chirped gratings for the in-plane geometry.

6. SUMMARY

We have described recent advances in key technology areas for Constellation-X reflection grating development. The feasibility of our modular assembly approach utilizing reference surfaces and alignment microcombs has been demonstrated. Since a major contribution to the error budget comes from the non-flatness of thin foils, it is our goal to improve assembly repeatability and accuracy within a module further. This will allow the foils to be as thin and therefore as light as possible. A major effort in our group is currently directed towards the problem of holding thin foils in a quasi-force-free state for repeatable and accurate foil shape metrology.[3,4,39] Naturally, reliable and accurate metrology is a prerequisite for improvements in foil shaping.

The process for the fabrication of microcombs was improved. We plan to reevaluate assembly truss repeatability and accuracy with the latest generation of microcombs.

We applied our experience gained in the fabrication of high-efficiency in-plane reflection gratings to producing blazed gratings for the off-plane geometry. Early efficiency measurements of our first off-plane gratings are very encouraging, but still leave room for improvement. Fine-tuning of the groove profile with feedback from simulations and AFM and x-ray measurements should lead to even higher diffraction efficiency. Manufacturability therefore does not weigh heavily anymore in the comparison between in-plane and off-plane geometries. For grating replication we will further investigate various nanoimprint lithography techniques.

With the Nanoruler we are in possession of a unique, fast, and highly accurate large-area grating patterning and metrology tool. The generation of variable period grating patterns as required for Constellation-X will be possible with the implementation of VP-SBIL.

ACKNOWLEDGMENTS

We gratefully acknowledge outstanding technical support from R. Fleming, E. Murphy, J. Carter, and J. Daley, as well as facility support from the NanoStructures Laboratory and the Microsystems Technology Laboratory at MIT. We also thank R. L. McEntaffer, S. Osterman, and W. C. Cash for making the data in Table 2 available to us. This work is supported by NASA grants NAG5-12583, NCC5-719, and NAG5-5405, and DARPA grants DAAG55-98-1-0130 and DAAD19-02-1-0204.

REFERENCES

1. M. C. Weisskopf, B. Brinkman, C. Canizares, G. Garmire, S. Murray, and L. P. Van Speybroeck, "An overview of the performance and scientific results from the Chandra x-ray observatory," *PASP* **114**, pp. 1–24, 2002.
2. http://constellation.gsfc.nasa.gov/
3. C. R. Forest, *X-ray Telescope Foil Optics: Assembly, Metrology, and Constraint*, Master's thesis, Dept. of Mechanical Engineering, MIT, 2003.
4. C. R. Forest, M. L. Schattenburg, C. G. Chen, R. K. Heilmann, P. T. Konkola, J. Przbylowski, Y. Sun, J. You, S. M. Kahn, and D. Golini, "Precision shaping, assembly, and metrology of foil optics for x-ray reflection gratings," in *X-ray and Gamma-ray Telescopes and Instruments for Astronomy*, J. E. Trümper and H. D. Tananbaum, eds., *Proc. SPIE* **4851**, pp. 538–548, 2003.
5. C. G. Chen, L. M. Cohen, R. K. Heilmann, P. T. Konkola, O. Mongrard, G. P. Monnelly, and M. L. Schattenburg, "Micro-comb design and fabrication for high accuracy optical assembly," *J. Vac. Sci. Technol. B* **18**, pp. 3272–3276, 2000.
6. G. P. Monnelly, D. Breslau, N. Butler, C. G. Chen, L. M. Cohen, W. Gu, R. K. Heilmann, P. T. Konkola, O. Mongrard, G. R. Ricker, and M. L. Schattenburg, "High-accuracy x-ray foil optic assembly," in *X-Ray Optics, Instruments, and Missions IV*, R. B. Hoover and A. B. Walker, eds., *Proc. SPIE* **4138**, pp. 164–173, 2000.

7. C. G. Chen, *Microcomb Fabrication for High Accuracy Foil X-ray Telescope Assembly and Vector Gaussian Beam Modeling*, Master's thesis, Dept. of Electrical Engineering and Computer Science, MIT, 2000.
8. O. Mongrard, *High-Accuracy Foil Optics for X-ray Astronomy*, Master's thesis, Dept. of Aeronautics and Astronautics, MIT, 2001.
9. O. Mongrard, N. Butler, C. G. Chen, R. K. Heilmann, P. T. Konkola, M. McGuirk, G. Monnelly, G. S. Pati, G. R. Ricker, M. L. Schattenburg, and L. Cohen, "High precision assembly and metrology of x-ray foil optics," in *Proceedings of the 16th Annual Meeting, The American Society for Precision Engineering* **25**, pp. 40–43, 2001.
10. Y. Sun, R. K. Heilmann, C. G. Chen, M. J. Spenko, C. R. Forest, and M. L. Schattenburg, "Precision microcomb design and fabrication for x-ray optics assembly," *submitted to J. Vac. Sci. Technol. B* **21**, 2003.
11. E. G. Loewen and E. Popov, *Diffraction Gratings and Applications*, Marcel Dekker, Inc., New York, 1997.
12. W. Werner, "X-ray efficiencies of blazed gratings in extreme off-plane mountings," *Appl. Opt.* **16**, pp. 2078–2080, 1977.
13. P. Vincent, M. Nevière, and D. Maystre, "X-ray gratings: The GMS mount," *Appl. Opt.* **18**, pp. 1780–1783, 1979.
14. J. W. den Herder *et al.*, "Performance and results of the reflection grating spectrometers on-board XMM-Newton," in *X-Ray and Gamma-Ray Telescopes and Instruments for Astronomy*, J. E. Trümper and H. D. Tananbaum, eds., *Proc. SPIE* **4851**, pp. 196–207, 2003.
15. L. I. Goray, "Rigorous efficiency calculations for blazed gratings working in in-plane and off-plane mountings in the 5-50 Å wavelengths range," in *Optics for EUV, X-Ray, and Gamma-Ray Astronomy*, O. Citterio and S. L. O'Dell, eds., *Proc. SPIE* **5168**, (these proceedings).
16. W. C. Cash, "X-ray optics. 2: A technique for high resolution spectroscopy," *Appl. Opt.* **30**, pp. 1749–1759, 1991.
17. R. McEntaffer, W. Cash, and A. Shipley, "Off-plane gratings for Constellation-X," in *X-Ray and Gamma-Ray Telescopes and Instruments for Astronomy*, J. E. Trümper and H. D. Tananbaum, eds., *Proc. SPIE* **4851**, pp. 549–556, 2003.
18. A. E. Franke, M. L. Schattenburg, E. M. Gullikson, J. Cottam, S. M. Kahn, and A. Rasmussen, "Super-smooth x-ray reflection grating fabrication," *J. Vac. Sci. Technol. B* **15**, pp. 2940–2945, 1997.
19. C.-H. Chang, R. K. Heilmann, R. C. Fleming, J. Carter, E. Murphy, M. L. Schattenburg, T. C. Bailey, J. G. Ekerdt, R. D. Frankel, and R. Voisin, "Fabrication of saw-tooth diffraction gratings using nanoimprint lithography," *submitted to J. Vac. Sci. Technol. B* **21**, 2003.
20. R. L. McEntaffer, F. R. Hearty, B. Gleeson, and W. C. Cash, "An x-ray test facility for diffraction gratings," in *Optics for EUV, X-Ray, and Gamma-Ray Astronomy*, O. Citterio and S. L. O'Dell, eds., *Proc. SPIE* **5168**, (these proceedings).
21. A. P. Rasmussen *et al.*, "Grating arrays for high-throughput soft x-ray spectrometer," in *Optics for EUV, X-Ray, and Gamma-Ray Astronomy*, O. Citterio and S. L. O'Dell, eds., *Proc. SPIE* **5168**, (these proceedings).
22. R. L. McEntaffer, S. N. Osterman, W. C. Cash, J. Gilchrist, J. Flamand, B. Touzet, F. Bonnemason, and C. Brach, "X-ray performance of gratings in the extreme off-plane mount," in *Optics for EUV, X-Ray, and Gamma-Ray Astronomy*, O. Citterio and S. L. O'Dell, eds., *Proc. SPIE* **5168**, (these proceedings).
23. S. Y. Chou, P. R. Krauss, and P. J. Renstrom, "Imprint of sub-25 nm vias and trenches in polymers," *Appl. Phys. Lett.* **67**, pp. 3114–3116, 1995.
24. T. C. Bailey, B. J. Choi, M. Colburn, M. Meissl, S. Shaya, J. G. Ekerdt, S. V. Sreenivasan, and C. G. Willson, "Step and flash imprint lithography: Template surface treatment and defect analysis," *J. Vac. Sci. Technol. B* **18**, pp. 3572–3577, 2000.
25. J. Ferrera, M. L. Schattenburg, and H. I. Smith, "Analysis of distortion in interferometric lithography," *J. Vac. Sci. Technol. B* **14**, pp. 4009–4013, 1996.
26. M. L. Schattenburg, C. G. Chen, P. N. Everett, J. Ferrera, P. T. Konkola, and H. I. Smith, "Sub-100 nm metrology using interferometrically produced fiducials," *J. Vac. Sci. Technol. B* **17**, pp. 2692–2697, 1999.
27. P. T. Konkola, C. G. Chen, R. K. Heilmann, and M. L. Schattenburg, "Beam steering system and spatial filtering applied to interference lithography," *J. Vac. Sci. Technol. B* **18**, pp. 3282–3286, 2000.

28. R. K. Heilmann, P. T. Konkola, C. G. Chen, G. S. Pati, and M. L. Schattenburg, "Digital heterodyne interference fringe control system," *J. Vac. Sci. Technol. B* **19**, pp. 2342–2346, 2001.
29. C. G. Chen, P. T. Konkola, R. K. Heilmann, G. S. Pati, and M. L. Schattenburg, "Image metrology and system controls for scanning beam interference lithography," *J. Vac. Sci. Technol. B* **19**, pp. 2335–2341, 2001.
30. C. G. Chen, R. K. Heilmann, C. Joo, P. T. Konkola, G. S. Pati, and M. L. Schattenburg, "Beam alignment for scanning beam interference lithography," *J. Vac. Sci. Technol. B* **20**, pp. 3071–3074, 2002.
31. C. G. Chen, P. T. Konkola, R. K. Heilmann, C. Joo, and M. L. Schattenburg, "Nanometer-accurate grating fabrication with scanning beam interference lithography," in *Nano- and Microtechnology: Materials, Processes, Packaging, and Systems*, D. K. Sood, ed., *Proc. SPIE* **4936**, pp. 126–134, 2002.
32. P. T. Konkola, *Design and Analysis of a Scanning Beam Interference Lithography System for Patterning Gratings with Nanometer-Level Distortions*, Ph. D. thesis, Dept. of Mechanical Engineering, MIT, 2003.
33. C. G. Chen, *Beam Alignment and Image Metrology for Scanning Beam Interference Lithography - Fabricating Gratings with Nanometer Phase Accuracy*, Ph. D. thesis, Dept. of Electrical Engineering and Computer Science, MIT, 2003.
34. P. T. Konkola, C. G. Chen, R. K. Heilmann, C. Joo, J. C. Montoya, C.-H. Chang, and M. L. Schattenburg, "Nanometer-level repeatable metrology using the Nanoruler," *submitted to J. Vac. Sci. Technol. B* **21**, 2003.
35. W. C. Cash, "X-ray spectrographs using radial groove gratings," *Appl. Opt.* **22**, pp. 3971–3976, 1983.
36. M. C. Hettrick, "Aberrations of varied line-space grazing incidence gratings in converging light beams," *Appl. Opt.* **23**, pp. 3221–3235, 1984.
37. M. L. Schattenburg, C. G. Chen, R. K. Heilmann, P. T. Konkola, and G. S. Pati, "Progress toward a general grating pattern technology using phase-locked scanning beams," in *Optical Spectrocopic Techniques and Instrumentation for Atmospheric and Space Research IV*, S. C. Barden and M. G. Mlynczak, eds., *Proc. SPIE* **4485**, pp. 378–384, 2002.
38. G. S. Pati, R. K. Heilmann, P. T. Konkola, C. Joo, C. G. Chen, E. Murphy, and M. L. Schattenburg, "A generalized scanning beam interference lithography system for patterning gratings with variable period progression," *J. Vac. Sci. Technol. B* **20**, pp. 2617–2621, 2002.
39. C. R. Forest, M. Akilian, G. Vincent, A. Lamure, and M. L. Schattenburg, "Thin glass optic and silicon wafer deformation and kinematic constraint," *submitted to Proceedings of the 18th Annual Meeting, The American Society for Precision Engineering* **29**, 2003.